Molecular Therapy
Methods & Clinical Development
Original Article

AAV9-NGLY1 gene replacement therapy improves phenotypic and biomarker endpoints in a rat model of NGLY1 Deficiency

Lei Zhu,[1] Brandon Tan,[1] Selina S. Dwight,[1] Brendan Beahm,[1] Matt Wilsey,[1] Brett E. Crawford,[1] Becky Schweighardt,[1] Jennifer W. Cook,[1] Thomas Wechsler,[1] and William F. Mueller[1]

[1]Grace Science, LLC, Menlo Park, CA 94025, USA

N-glycanase 1 (NGLY1) Deficiency is a progressive, ultra-rare, autosomal recessive disorder with no approved therapy and five core clinical features: severe global developmental delay, hyperkinetic movement disorder, elevated liver transaminases, alacrima, and peripheral neuropathy. Here, we confirmed and characterized the *Ngly1*$^{-/-}$ rat as a relevant disease model. GS-100, a gene therapy candidate, is a recombinant, single-stranded adeno-associated virus (AAV) 9 vector designed to deliver a functional copy of the human *NGLY1* gene. Using the *Ngly1*$^{-/-}$ rat, we tested different administration routes for GS-100: intracerebroventricular (ICV), intravenous (IV), or the dual route (IV + ICV). ICV and IV + ICV administration resulted in widespread biodistribution of human NGLY1 DNA and corresponding mRNA and protein expression in CNS tissues. GS-100 delivered by ICV or IV + ICV significantly reduced levels of the substrate biomarker N-acetylglucosamine-asparagine (GlcNAc-Asn or GNA) in CSF and brain tissue compared with untreated *Ngly1*$^{-/-}$ rats. ICV and IV + ICV administration of GS-100 resulted in behavioral improvements in rotarod and rearing tests, whereas IV-only administration did not. IV + ICV did not provide additional benefit compared with ICV administration alone. These data provide evidence that GS-100 could be an effective therapy for NGLY1 Deficiency using the ICV route of administration.

INTRODUCTION

N-glycanase 1 (NGLY1) Deficiency is a progressive, debilitating, ultra-rare autosomal recessive disorder with approximately 100 patients identified worldwide to date. With no approved therapy,[1] treatment is focused on the management of the severe and progressive symptoms, in particular the six core features of the disease: severe global developmental delay, a hyperkinetic movement disorder, elevated liver transaminases, (hypo)-alacrima (inability to produce tears), peripheral neuropathy, and global accumulation of N-acetylglucosamine-asparagine (GlcNAc-Asn or GNA).[2–6] Many affected individuals also require constant daily care and frequent hospitalizations for persistent medical issues.[2]

NGLY1 Deficiency is caused by loss-of-function mutations in the *NGLY1* gene,[2] which encodes the NGLY1 protein, a ubiquitous cytosolic N-glycanase implicated in the endoplasmic-reticulum-associated protein degradation (ERAD) pathway that recognizes and eliminates unfolded or incorrectly processed glycoproteins. Specifically, NGLY1 removes *N*-linked glycans from misfolded proteins en route to the proteasome for degradation.[3] This is done by hydrolyzing the N-acetylglucosamine-asparagine (GlcNAc-Asn) bond linking the glycan to the protein and liberating the *N*-glycan in the process. In the absence of NGLY1, there are no alternative mechanisms for cleaving this bond in the cytosol, thus the glycan is cleaved at an alternative bond leaving a partially deglycosylated protein that retains the GlcNAc-Asn bond. While the rest of the released glycan can be processed and then transported to and degraded in the lysosome, the GlcNAc-retaining protein is degraded by the proteasome to peptides, then further degraded to amino acids and GlcNAc-Asn. GlcNAc-Asn (GNA) is the primary substrate biomarker of NGLY1 Deficiency, as its accumulation is directly related to the absence of NGLY1 function; this accumulation can be measured in the plasma, urine,[3,7] and dried blood spots of NGLY1 Deficiency patients.[8]

A rat model of NGLY1 Deficiency was created and characterized by Tadashi Suzuki's group.[9] It was found to exhibit key similarities to human NGLY1 Deficiency phenotypes: reduced survival and fitness, peripheral axonal neuron loss, neurological impairment, motor dysfunction, and impaired spatial learning in the rat model which are analogous to failure to thrive, peripheral neuropathy, hyperkinetic movements, and delayed cognitive development in humans.[9] Many of these deficits likely originate from the central nervous system (CNS) and peripheral nervous system (PNS).

Here, we report the results of a newly developed gene replacement therapy, GS-100, for the treatment of NGLY1 Deficiency in the *Ngly1*$^{-/-}$ rat model using our quantitative, targeted assay to analyze GNA levels in plasma, urine, and CSF samples.[7] GS-100 is a recombinant single-stranded adeno-associated virus subtype 9 (AAV9)

Received 31 March 2022; accepted 29 September 2022;
https://doi.org/10.1016/j.omtm.2022.09.015.

Correspondence: William F. Mueller, Grace Science, LLC, 1142 Crane Street, Ste 4, Menlo Park, CA 94025, USA.
E-mail: Will@gracescience.com

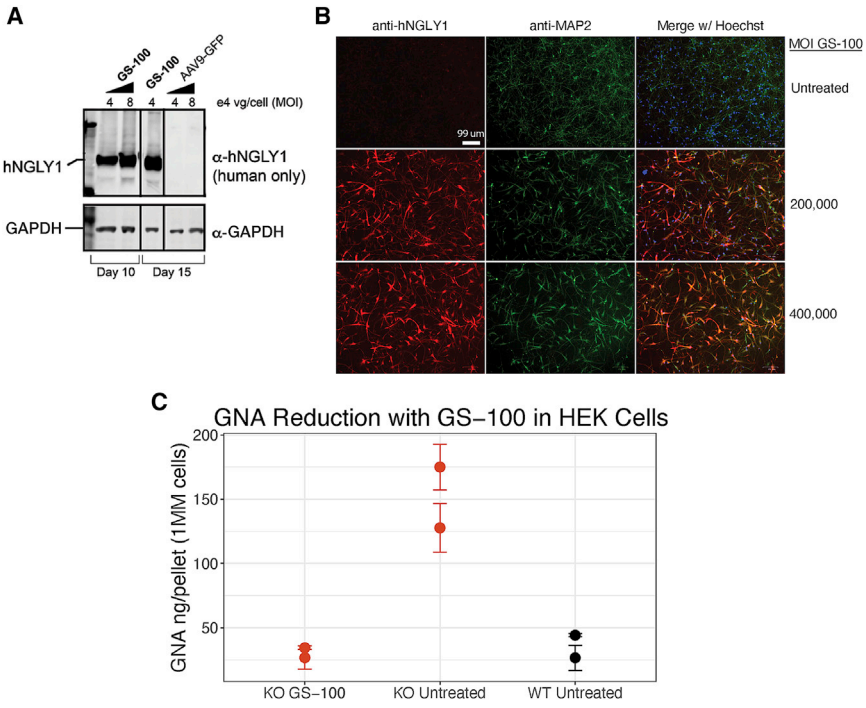

Figure 1. *In vitro* expression of NGLY1 in neuronal cultures and reduction of GNA in *NGLY1*$^{-/-}$ HEK293 cells after GS-100 transduction

(A) *In vitro* expression of NGLY1 protein in rat primary neurons following GS-100 transduction. Rat primary neurons were transduced with GS-100 or AAV9-GFP control at 40,000 or 80,000 multiplicity of infection (MOI) 5 days after plating. The neurons were lysed 5 days (day 10 of the experiment) or 10 days (day 15 of the experiment) after transduction, and human NGLY1 protein was probed by western blot. GAPDH was used as the loading control. (B) *NGLY1*$^{-/-}$ ReNcell VM neurons were transduced with GS-100 at 0, 200,000, or 400,000 MOI 5 days after differentiation. Cells were fixed and probed for NGLY1 (red) or MAP2 (green) expression using immunofluorescence 7 days after transduction. Cell nuclei were stained with Hoechst 33342 blue dye. (C) Reduction of GNA in *NGLY1*$^{-/-}$ HEK293 cells after GS-100 transduction. *NGLY1*$^{-/-}$ HEK293 cells were transduced with GS-100 at 300,000 MOI and cell lysates were harvested 72 h after transduction. GNA levels in the lysate were measured and normalized to the number of cells. Each data point represents an experiment and error bars show the standard deviation. AAV9, adeno-associated virus 9; GAPDH, glyceraldehyde 3-phosphate dehydrogenase; GFP, green fluorescent protein; GNA, GlcNAc-Asn; KO, knockout; MAP2, microtubule-associated protein 2; MOI, multiplicity of infection; NGLY1, *N*-glycanase 1.

vector that encodes a codon-optimized full-length version of the human *NGLY1* gene driven by a CAG-derived ubiquitous promoter. GS-100 is distinct from the AAV9-CMV-*hNGLY1* vector used by Asahina et al. because GS-100 utilizes CAG rather than CMV and the gene encoded is codon optimized rather than the wild-type (WT) *hNGLY1* gene.[1] GS-100 transduction resulted in higher hNGLY1 expression than the non-codon-optimized AAV-CAG-*hNGLY1* in HEK293 cells and in rat neurons (data not shown). We evaluated the efficacy and safety of GS-100 delivered to the *Ngly1*$^{-/-}$ rats via three routes of administration: intracerebroventricular (ICV), intravenous (IV), or a dual route (IV + ICV). IV and ICV routes have both been used to deliver other AAV9 gene therapies to the brain in clinical and non-clinical studies.[10,11] At 3, 5, 7, and 9 weeks after GS-100 administration, we evaluated motor function and behavior using rotarod and locomotor (rearing) tests and compared the behavioral results across these three routes of administration. At the end of the study, we evaluated *hNGLY1* DNA biodistribution, *hNGLY1* mRNA expression, *hNGLY1* protein expression, and GNA biomarker from animals treated with GS-100 via the three different routes. These data demonstrated that ICV administration is the preferred route of delivery for GS-100 as a therapy for NGLY1 Deficiency.

RESULTS

Ngly1 knockout rat generation and phenotypes

An *Ngly1* knockout (KO) Sprague-Dawley rat model was generated and characterized by Asahina et al.[9] We established a colony of these rats to confirm the model phenotypes and test GS-100. Our characterization study confirmed the majority of phenotypes previously observed in the *Ngly1*$^{-/-}$ rat model, including reduced survival ratio (19.87% versus 100% for WT and *Ngly1*$^{+/-}$), decreased body weight gain in males (Figure S1), deteriorating performance in rotarod and rearing tests (N = 14, Figure S2), and deficits in the functional observational battery (FOB) test (Figure S3).[9,12–14]

In vitro validation of the NGLY1 gene therapy candidate, GS-100

Human NGLY1 was detected in the lysate of primary cortical rat neurons as early as 5 days after GS-100 transduction, and the expression of hNGLY1 increased with either time or multiplicity of infection (MOI) (Figure 1A). Widespread hNGLY1 expression was detected 7 days after GS-100 transduction in human neurons, and most NGLY1-expressing cells were also positive for the neuronal marker MAP2 (Figure 1B). These results suggest that GS-100 can effectively transduce neuronal cells and express hNGLY1 *in vitro*. Levels of the biomarker GNA in *NGLY1*$^{-/-}$ neuronal cells were found to be normalized to WT HEK293 cell levels 72 h after GS-100 transduction (Figure 1C), demonstrating that GS-100 transduction results in expression of functional hNGLY1 protein and that restoring NGLY1 activity is directly responsible for the correction of biomarker GNA levels.

In vivo validation of NGLY1 gene therapy and optimal route of administration

To determine the optimal route of administration to deliver GS-100 to the CNS, we administered GS-100 to *Ngly1*$^{-/-}$ rats through IV,

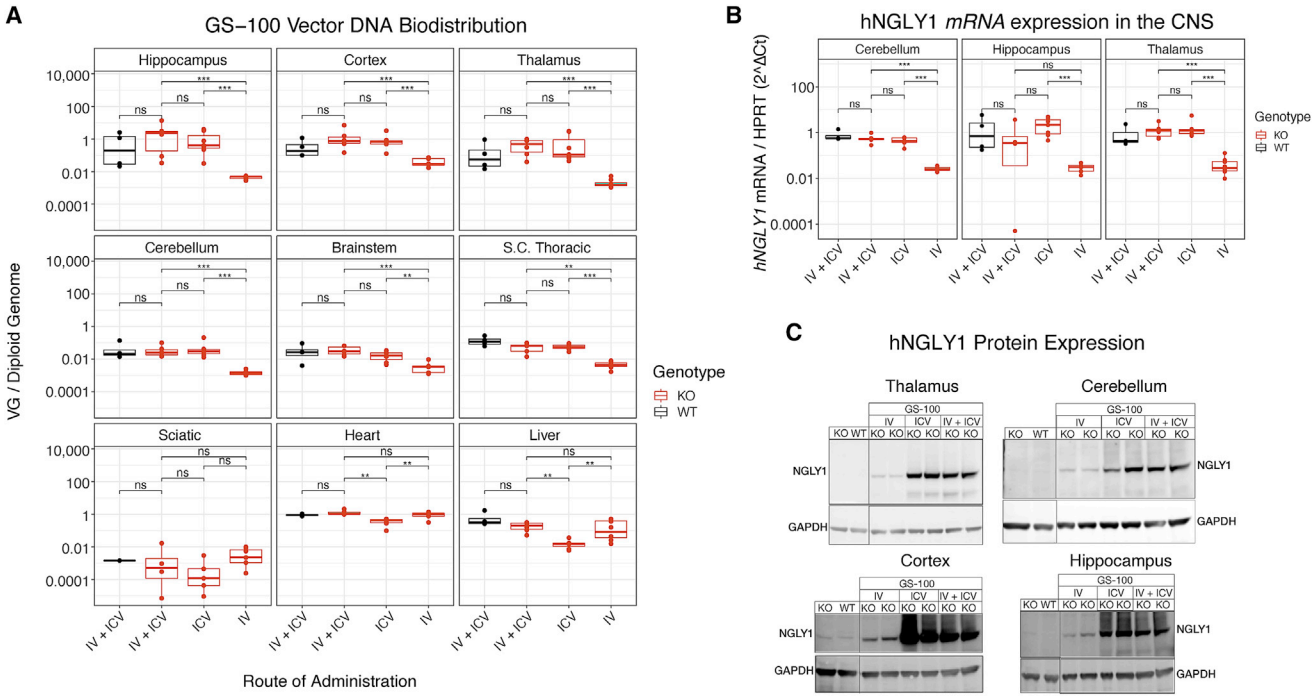

Figure 2. DNA biodistribution and expression (mRNA and protein) of the *NGLY1* transgene after *in vivo* transduction using three routes of administration

(A) Biodistribution of GS-100 in CNS tissues by genotype when dosed via the IV, ICV, or dual IV + ICV route. Total DNA was extracted from each specified CNS tissue. Viral genome (vg) DNA was quantified against input DNA amount and a GS-100 vector genome plasmid standard. The resulting data were plotted per route of administration, genotype, and tissue. Minimum of four animals per group, each point represents one animal. *p < 0.05, **p < 0.01, ***p < 0.001. (B) Human *NGLY1* mRNA detection in CNS tissue following GS-100 administration via the IV, ICV, or dual IV + ICV route. RT-qPCR was performed on mRNA isolated from each specific CNS tissue and relative cDNA levels were calculated using the ΔCt method using the housekeeping gene *HPRT* as internal control. Minimum of four animals per group, each point represents one animal. *p < 0.05, **p < 0.01, ***p < 0.001. (C) Human NGLY1 protein expression by western blot in cortex, hippocampus, thalamus, and cerebellum after GS-100 dosing via the IV, ICV, or dual IV + ICV route. The antibody used in this study recognizes human NGLY1 protein but not the endogenous rat Ngly1 protein. GAPDH, glyceraldehyde 3-phosphate dehydrogenase; hNGLY1, human *NGLY1*; KO, knockout; ICV, intracerebroventricular); IV, intravenous; NGLY1, *N*-glycanase 1; S.C., spinal cord.

ICV, or the dual route of IV + ICV. After IV, ICV, and IV + ICV dosing of GS-100 at postnatal day (PND) 35–49, the *Ngly1*$^{-/-}$ rats did not exhibit any adverse effects related to surgery or GS-100 as assessed by cage-side observation. At the end of the 9-week study, the hippocampus, cortex, and thalamus had the highest levels of *hNGLY1* DNA (Figure 2A) following administration by ICV or IV + ICV. *hNGLY1* DNA detected in CNS tissue was significantly lower in the IV group compared with ICV or IV + ICV groups, except for the cortex, where a slightly higher signal was observed. There was no evidence of an additive or synergistic effect of IV administration in the IV + ICV route (Figure 2A). GS-100 transduction in the heart was comparable across all routes of administration (Figure 2A). GS-100 transduction efficiency in the liver was higher for IV administration than for ICV (Figure 2A), as expected. The sciatic nerve showed very low, highly variable GS-100 transduction. Similar to the vector DNA biodistribution results, h*NGLY1* mRNA expression was significantly higher in CNS tissues when GS-100 was administered by either ICV or IV + ICV versus IV administration (Figure 2B). The h*NGLY1* mRNA expression data in the thalamus, hippocampus, and cerebellum were consistent with the vector DNA genome levels observed in CNS tissues (Figures 2A and 2B).

hNGLY1 protein expression was assessed by western blot and was highest in the cortex and hippocampus in ICV-dosed groups (Figure 2C). ICV delivery also resulted in high levels of hNGLY1 protein expression in the thalamus and cerebellum, whereas IV administration resulted in low hNGLY1 protein expression in these brain regions. There was no evidence of an additive or synergistic effect of IV administration in the dual route of IV + ICV, as was the case with *hNGLY1* DNA biodistribution and mRNA expression. Expression in the heart (Figure S4) was consistent with DNA biodistribution data. Human NGLY1 protein expression was undetectable in the liver (data not shown).

Human NGLY1 protein expression in brain detected by immunohistochemistry

Widespread hNGLY1 protein expression was detected by immunohistochemistry (IHC) in the brains of rats dosed with GS-100 via ICV and IV + ICV, while lower NGLY1 protein expression was observed in the IV-dosed group (Figure 3). Similar to biodistribution and mRNA expression (Figure 2), there was not a substantial increase in the number of hNGLY1-positive cells in the

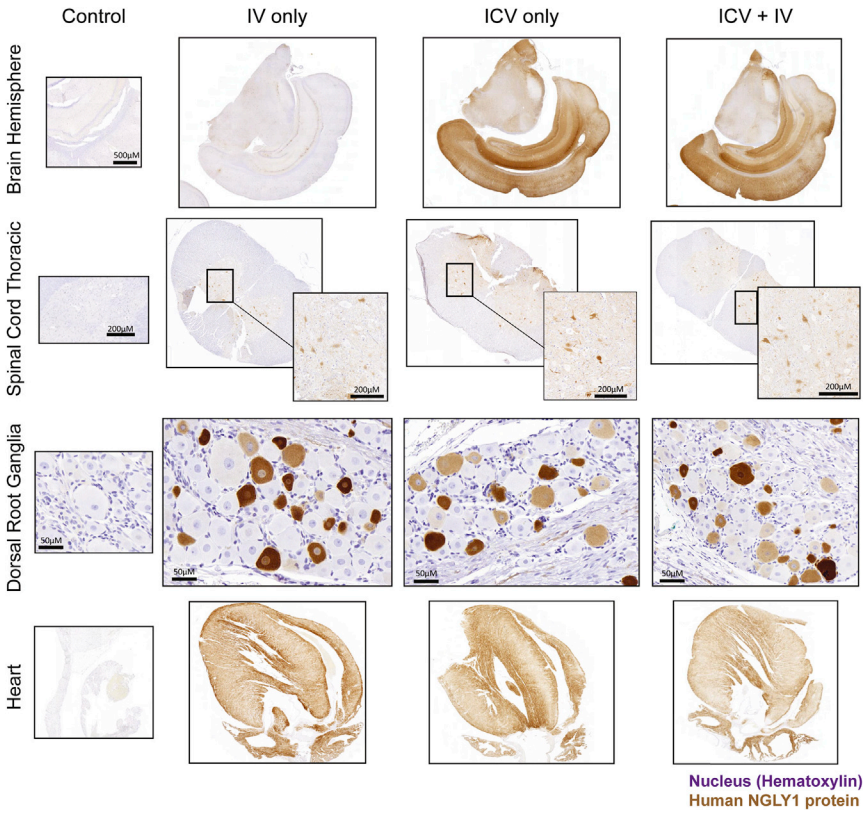

Figure 3. hNGLY1 expression in the brain, heart, spinal cord (thoracic), and DRG by IHC 9 weeks after GS-100 delivery via different routes of administration

IHC was performed on fixed tissue slices using NGLY1 antibody, and representative images of the brain, spinal cord (thoracic), DRGs, and heart tissue slices 9 weeks after dosing are shown. Hematoxylin staining was used as a nucleus counterstain. Zoomed-in images show NGLY1 staining in the ventral horn of the spinal cord.

CNS of the IV + ICV group compared with the ICV group, indicating little to no contribution of IV administration to hNGLY1 protein expression in the brain (Figure 3). All three routes achieved similar expression in the spinal cord. A slightly higher percentage of NGLY1-positive cells was observed in the dorsal root ganglion (DRG) of rats injected via the IV + ICV route than via ICV alone, which is not surprising given the DRG is located outside of the blood-brain barrier (BBB) (Table 1; Figure 3). Human NGLY1 expression was localized in the cell bodies of the dorsal and ventral horn in the spinal cord. All three routes resulted in similar hNGLY1 protein expression in the heart (Figure 3).

The percentage of cells expressing hNGLY1 protein after IV administration alone was low across all CNS tissues (0.03%–1.95% cells positive for hNGLY1 protein staining, Table 1). ICV delivery of GS-100 resulted in a considerably higher percentage of cells expressing hNGLY1 protein in the CNS, with the highest percentage in the cerebral cortex (12%), hippocampus (15%), and thalamus (11%) (Table 1). In brainstem, cerebellum, and striatum, the number of hNGLY1-positive cells was less than 3% (Table 1), but image analysis of the cerebellum revealed highly localized hNGLY1 expression in Purkinje and stellate cells, important for motor coordination, following ICV administration of GS-100 (Figure S5). Compared with the ICV group, GS-100 delivery via the IV + ICV route resulted in a higher percentage of hNGLY1-positive cells in the DRG and spinal cord but only a marginally higher percentage in the brain (Table 1).

GNA biomarker levels decrease in CSF, blood, and tissues following GS-100 dosing

Untreated *Ngly1*$^{-/-}$ rats had increased GNA biomarker levels in CSF, plasma, and PNS and CNS tissues compared with WT rats (Figure 4). GNA levels of ICV or IV + ICV-treated groups collected at the 9-week terminal time point demonstrated an average decrease of 23% in the plasma and 30% in the CSF compared with untreated *Ngly1*$^{-/-}$ rats (Figure 4A). IV administration did not significantly decrease CSF GNA levels (Figure 4A) compared with untreated *Ngly1*$^{-/-}$ controls, consistent with the lack of GS-100 DNA biodistribution and *hNGLY1* mRNA or protein expression observed in the same group.

ICV and IV + ICV GS-100-treated groups showed a significant GNA reduction in the cortex, hippocampus, and thalamus (>50%), while no significant reduction was observed in those CNS tissues in the IV GS-100-treated group (Figure 4C). Both cerebellum and brain stem also showed significant reduction of GNA by ∼30% in *Ngly1*$^{-/-}$ rats dosed with GS-100 via ICV delivery compared with untreated *Ngly1*$^{-/-}$ rats (calculated from GNA concentrations as shown in Figure 4C). GNA reduction in the spinal cord (thoracic) was about 15%–20% for each of the three administration routes tested (Figure 4C). GNA reduction in the heart was >50%, while reduction in liver and sciatic nerve tissue averaged <20% for all routes (Figure 4B). Except for the heart, peripheral tissues exhibited variable GNA reduction, independent of the route of administration.

GS-100 DNA transduction levels correlated positively with *hNGLY1* mRNA levels (Figures 5A and 5D) in the thalamus and hippocampus. GS-100 transduction levels (Figures 5C and 5F) and h*NGLY1* mRNA levels (Figures 5C and 5F) correlated with GNA reduction in the thalamus and hippocampus. Both CSF GNA levels (Figure 5G) and average CNS tissue GNA (Figure 5H) correlated negatively with the percentage of hNGLY1-positive cells in the same CNS regions. The strong negative correlation between hNGLY1 DNA (and mRNA,

Table 1. Immunohistochemical quantification of NGLY1-positive cells in subregions of the brains of animals dosed via IV, ICV, or dual IV + ICV routes of administration

Brain region	NGLY1-positive cells as measured by IHC following GS-100 delivery via different routes of administration (%)		
	ICV	IV	IV + ICV
DRGs	16.26	26.58	34.75
Spinal cord	27.62	15.29	34.79
Thalamus	11.38	1.15	12.32
Hypothalamus	2.79	0.16	2.57
Hippocampus	15.26	1.23	20.05
Cerebral cortex	11.90	0.58	15.32
Brainstem[a]	1.89	0.58	2.00
Cerebellum[b]	1.54	0.10	2.05
Striatum[c]	2.94	0.32	2.53

The percentage of human NGLY1-positive cells for different tissues was calculated by normalizing the number of human NGLY1-positive cells to the total number of cells in the same region, as identified by hematoxylin staining.
[a]Including medulla and rostral midbrain.
[b]The granule cell layer is excluded in the quantification due to the densely packed nature.
[c]Including caudate/putamen and nucleus accumbens. ICV, intracerebroventricular; IV, intravenous; NGLY1, *N*-glycanase 1.

protein) with GNA biomarker demonstrates pharmacodynamic effect of GS-100 in the *Ngly1*$^{-/-}$ rats.

Amelioration of motor and neurobehavioral deficits after GS-100 ICV administration

In the rotarod test, the latency to fall assessed at 3, 5, 7, and 9 weeks after GS-100 administration was significantly lower ($p = 0.013$) in untreated *Ngly1*$^{-/-}$ rats compared with WT controls (Figure 6A), consistent with results from the characterization study (Figure S2A) and those of Asahina et al.[9] *Ngly1*$^{-/-}$ rats dosed with GS-100 via the ICV or dual IV + ICV routes showed significant improvement ($p = 0.0022$ [ICV] and $p = 0.019$ [IV + ICV]). All analysis used a generalized linear model, considering genotype, treatment, routes, and time factor from week 3 through week 9 compared with untreated *Ngly1*$^{-/-}$ controls (Figure 6A). No significant improvement was observed when comparing *Ngly1*$^{-/-}$ rats treated via the IV route with untreated *Ngly1*$^{-/-}$ controls using the same statistical model. There was no additional significant improvement observed for the IV + ICV route over the ICV route. These data demonstrate that, even after the manifestation of motor deficits in *Ngly1*$^{-/-}$ rats (around 5 weeks postnatal; Figure S2A), rotarod test deficits can be improved after ICV dosing of GS-100.

When comparing untreated *Ngly1*$^{-/-}$ rats with WT rats in the open-field test, we observed a significant decrease in the number of rearing ($p < 0.05$, one-way ANOVA with Sidak's after test comparison) in the *Ngly1*$^{-/-}$ rats (Figure 6B), similar to the characterization study (Figure S2B). *Ngly1*$^{-/-}$ rats treated with GS-100 via the ICV route or dual IV + ICV route showed statistically significant improvement over untreated control *Ngly1*$^{-/-}$ animals 6 weeks after GS-100 administration ($p < 0.001$ and $p < 0.001$, one-way ANOVA with Sidak's after test comparison, respectively), while IV delivery of GS-100 showed no clear benefit over control.

To analyze whether biomarker reduction correlates with behavioral improvement, the GNA levels in CSF and CNS tissues were compared with rearing in the open field in *Ngly1*$^{-/-}$ animals. A correlation analysis between rearing activity and CSF GNA levels revealed a significant negative correlation ($R^2 = 0.38$, $p = 0.0002$) (Figure 6C) between the number of rearing and CSF GNA levels of individual *Ngly1*$^{-/-}$ animals. In addition, a significant negative correlation between rearing activity and GNA levels averaged across CNS tissues (hippocampus, cortex, brainstem, and thalamus) was detected in *Ngly1*$^{-/-}$ animals ($R^2 = 0.46$, $p < 0.0001$) (Figure 6D). These analyses demonstrate that GNA substrate biomarker levels in the CSF and CNS tissues correlate with behavioral improvement in GS-100-treated animals, providing evidence that GNA levels could be used to assess clinical benefit related to GS-100 treatment restoring NGLY1 function.

Safety of GS-100 administration

There was no significant elevation of ALT, AST, ALP, or total bilirubin levels following administration (Figure S6), regardless of the route. There were no macroscopic pathology findings attributable to GS-100. Histopathological findings included localized hippocampal neuronal loss and gliosis adjacent to the needle track in both GS-100 and vehicle ICV-dosed groups. These localized findings were attributed to the spatial constraints of administering into the small *Ngly1*$^{-/-}$ rat brain and are not expected to translate to humans. Minimal cell body degeneration and/or minimal to mild increases in satellite glial cellularity were noted in the DRGs at the cervical, thoracic, and/or lumbar levels of *Ngly1*$^{-/-}$ rats with no treatment and are considered to be a phenotype of *Ngly1*$^{-/-}$ rats. These DRG findings were not exacerbated by GS-100 treatment regardless of route of administration.

DISCUSSION

NGLY1 Deficiency is a rare, devastating disorder with no approved therapeutic options. Here we confirm characterization of an *Ngly1* KO rat animal model of NGLY1 Deficiency and demonstrate the efficacy of GS-100, an AAV9 NGLY1 gene therapy for NGLY1 Deficiency, to rescue functional and biochemical phenotypes of *Ngly1*$^{-/-}$ rats *in vitro* and *in vivo*.[7,9] The previously described biomarker GNA[7] shows consistent negative correlation with hNGLY1 DNA, mRNA, and protein expression in brain tissue and functional improvement. These findings provide evidence that GNA acts as a pharmacodynamic marker that correlates with treatment effect that may serve as a surrogate marker of clinical efficacy in GS-100 clinical trials.

Understanding potential routes of gene therapy administration is critical for correcting gene expression in target tissues. GS-100 delivered via ICV administration resulted in *hNGLY1* DNA biodistribution, mRNA, and protein expression in the CNS that correlated with GNA reduction and functional rescue in *Ngly1*$^{-/-}$ rats. IV dosing on

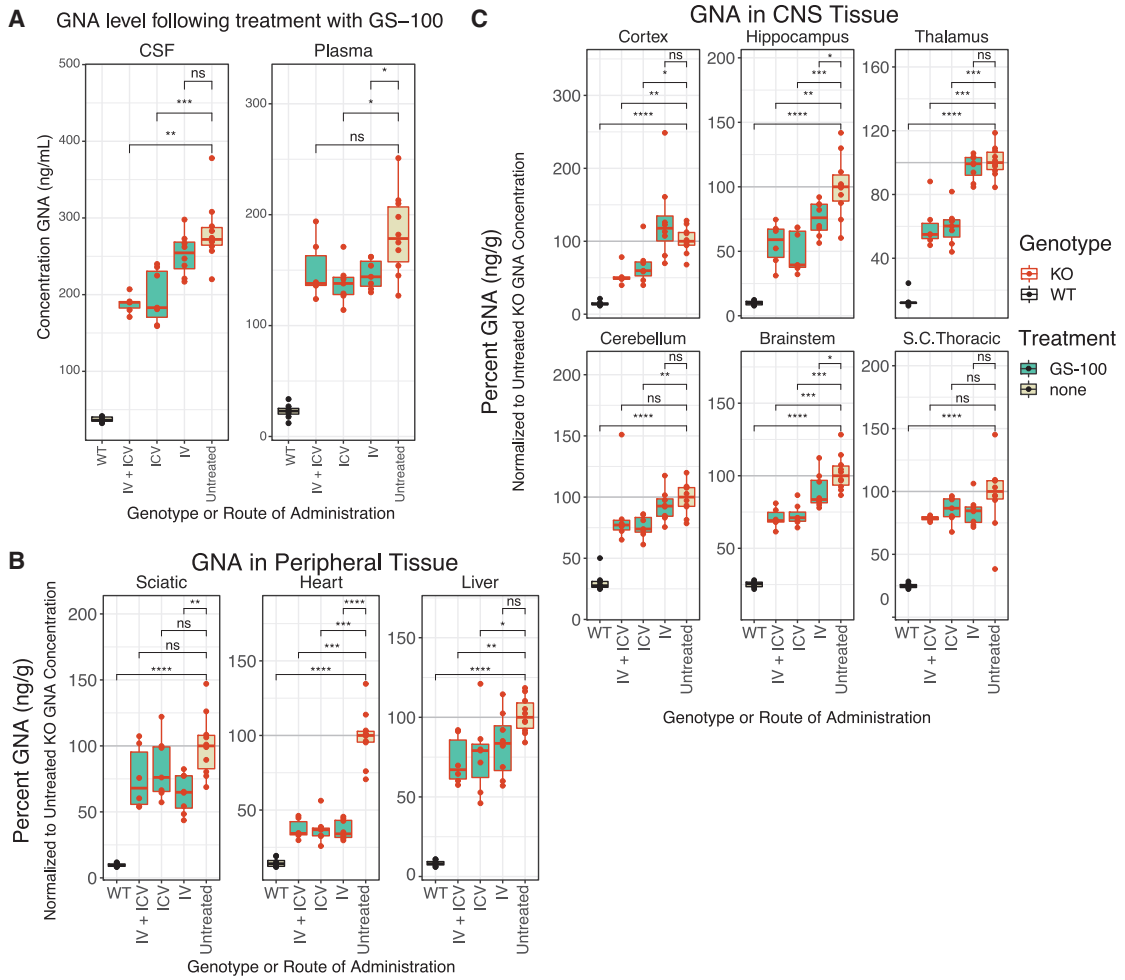

Figure 4. Changes in GNA levels in CSF, blood, CNS tissues, and peripheral tissues following treatment with GS-100

(A) Terminal GNA levels in the CSF and plasma following GS-100 administration using IV, ICV, or dual IV + ICV route of administration. CSF and blood samples were collected by intra-cisterna magna (ICM) syringe extraction or cardiac puncture, respectively and plotted per animal (each point represents one animal). *p < 0.05, **p < 0.01, ***p < 0.001. (B and C) GNA levels in peripheral (B)and CNS (C) tissues 9 weeks after treatment with GS-100 via the IV, ICV or IV + ICV route. GNA levels in each tissue were normalized to the median GNA concentration detected for untreated *Ngly1*$^{-/-}$ rats in the same tissue and plotted per animal (each point represents one animal). *p < 0.05, **p < 0.01, ***p < 0.001, ****p < 0.0001. GNA, GlcNAc-Asn; KO, knockout; ICV, intracerebroventricular; IV, intravenous; NGLY1, *N*-glycanase 1; WT, wild type.

its own did not restore neurobehavioral phenotypes, likely due to the significantly lower *hNGLY1* biodistribution and expression levels in the CNS compared with ICV or IV + ICV routes of administration. IV + ICV dosing provided no significant additional benefit beyond ICV dosing alone, consistent with other genetic CNS disease models treated with AAV.[15] ICV dosing allows for lower vector loads than systemic administration (IV) and may minimize potential safety issues seen in systemic dosing.[16]

Our results demonstrate that ICV dosing of GS-100 results in hNGLY1 expression in disease-relevant CNS regions, including the cerebral cortex, hippocampus, thalamus, cerebellum, spinal cord, and DRGs. The cerebral cortex and hippocampus are likely implicated in the global cognitive deficits and high-level motor symptoms observed in both NGLY1 Deficiency patients[2,4,6] and the rat model.[9] The absence of NGLY1 expression in the thalamus, cerebellum, and spinal cord likely contributes to the hyperkinetic movement disorder in patients[2,4,6] and motor function deficits in *Ngly1*$^{-/-}$ rats.[1,9] The DRGs and related peripheral nerves likely are involved in the peripheral neuropathy in NGLY1 Deficiency patients.[2,4,6] While GS-100 transduction and hNGLY1 protein expression were detected in each of the CNS and PNS regions mentioned above, hNGLY1 protein expression detected by immunohistochemistry (IHC) was lower than expected compared with the corresponding viral DNA biodistribution in these tissues. This could be due to IHC being a less quantitative method compared with PCR as there is often variability in detector antibody specificity and background signal sensitivity with the IHC method. The consistency between transduction, protein

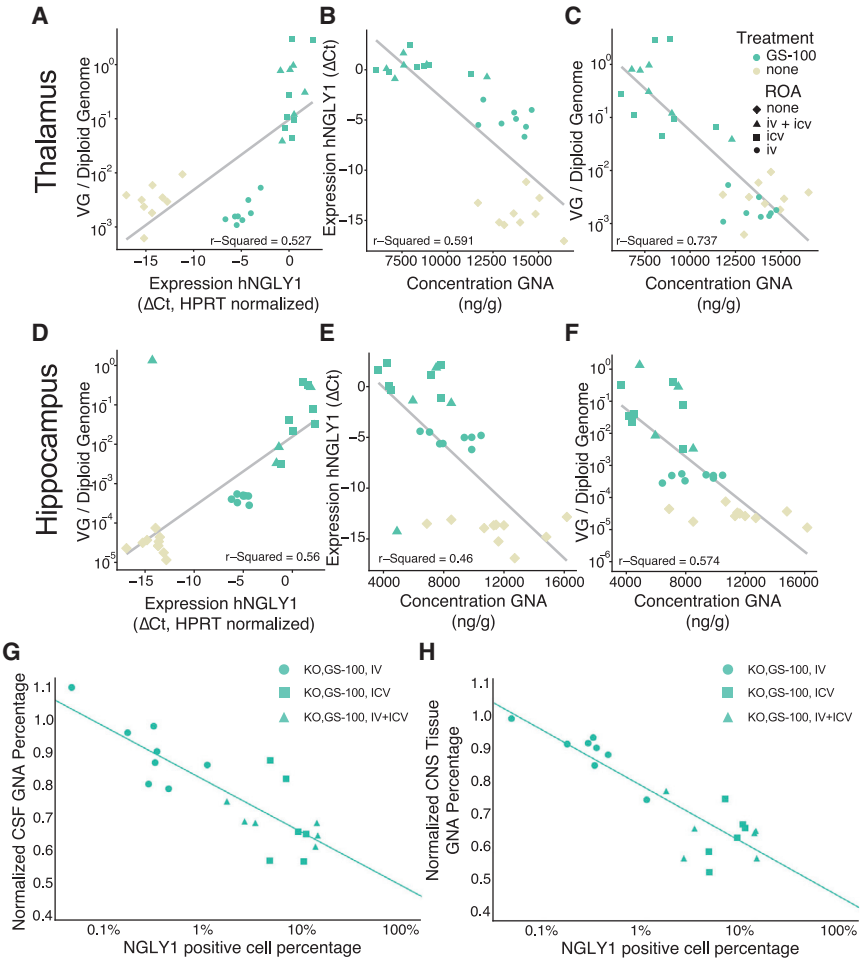

Figure 5. Correlation between GNA levels, vector transduction, *NGLY1* mRNA expression, and NGLY1 protein distribution in CNS tissues following GS-100 administration via different routes

(A–F) GNA concentration inversely correlates with GS-100 biodistribution/vector transduction and human *NGLY1* mRNA expression by log-linear correlation. (A and D) Vector transduction (vg/diploid genome) was plotted against *NGLY1* mRNA expression in the thalamus (A) and hippocampus (D). (B and E) *NGLY1* mRNA expression was plotted against GNA concentration in the thalamus (B) and hippocampus (E). (C and F) Vector transduction was plotted against GNA concentration in the thalamus (C) and hippocampus (F). Diamond, untreated; circle, IV route; square, ICV route; triangle, IV + ICV dual routes. Each point represents one animal. (G and H) Scaled GNA level inversely correlates with the number of positive cells in CNS tissues by linear correlation. Scaled GNA levels in the CSF (G) or in tissues (averaged GNA levels of hippocampus, cortex, brainstem, thalamus; H) are plotted against the percentage of NGLY1-positive cells of all cross-sections of the rat brain (R^2 = 0.71 and R^2 = 0.69, respectively). Scaled GNA levels were taken by averaging the GNA percentage reduction per tissue per animal and plotting that combined average against the NGLY1 percentage positive cell number for that same animal. Each point represents one animal. GNA, GlcNAc-Asn; ICV, intracerebroventricular; IV, intravenous; NGLY1, *N*-glycanase 1.

expression, and behavioral improvement data support ICV dosing as the preferred GS-100 administration route for future clinical trials.

It is difficult to directly compare the dose of a CSF delivery and dose via a systemic route like IV. Relatively high AAV9 doses were chosen for this study in the interest of showing efficacy for proof of concept. The high dose of 6×10^{12} vg/animal total used in the ICV route was based on high doses of AAV9 previously used for ICV administration in other non-clinical studies in mice and rat.[10,17] The IV dose of 1×10^{14} vg/kg is also close to some of the highest doses used in rodents.[10]

Because NGLY1 Deficiency is a relatively newly characterized disease,[6] limited clinical data pose a challenge for selecting clinical endpoints for future clinical trials. Our data demonstrate that GNA is a pharmacodynamic biomarker of GS-100 activity that correlates strongly with locomotor improvement and overall treatment benefit. Reduction in GNA levels in the plasma, CSF, and brain tissue correlated with delivery and expression of human NGLY1 as well as improvements in behavioral phenotypes. Although GNA levels in *Ngly1*$^{-/-}$ rats were reduced by GS-100 transduction, GNA of WT levels were not reached. This is likely due to the fact that NGLY1 is a cytosolic protein and cannot be shared between cells, requiring most, if not all, cells be transduced to completely restore a WT GNA profile.[7] Although a substantial percentage of cells were transduced and expressed hNGLY1 protein, not all cells of the brain were transduced, and therefore some amount of abnormal GNA is expected to persist. Our *in vitro* experiments in HEK cells (Figure 1C) demonstrated that GNA levels in *Ngly1*$^{-/-}$ cells can be reduced to WT levels if most cells have been transduced with GS-100 and express functional NGLY1 protein. Additional studies employing higher GS-100 doses are required to determine whether GNA levels can be further reduced following ICV administration. Given the behavioral improvements detected in this study, GNA reduction to WT levels may not be required for functional improvement in humans. Previous *in vitro* studies demonstrated that GNA biomarker levels in cells are directly linked to NGLY1 activity and that GS-100 transduction of NGLY1-deficient cells can normalize GNA substrate biomarker levels (Figure 1C; Mueller et al.).[7] Asahina et al. found that reduction in GNA biomarker in the spinal cord after ICV dosing correlated with phenotypic improvement.[9] However, that study did not analyze the biomarker in the brain or CSF and was therefore unable to correlate brain or CSF biomarker reduction with phenotype improvement. The data from Asahina et al.[9] combined with the data in this study suggest that small GNA reductions could correlate with positive phenotypic outcomes in the clinic.

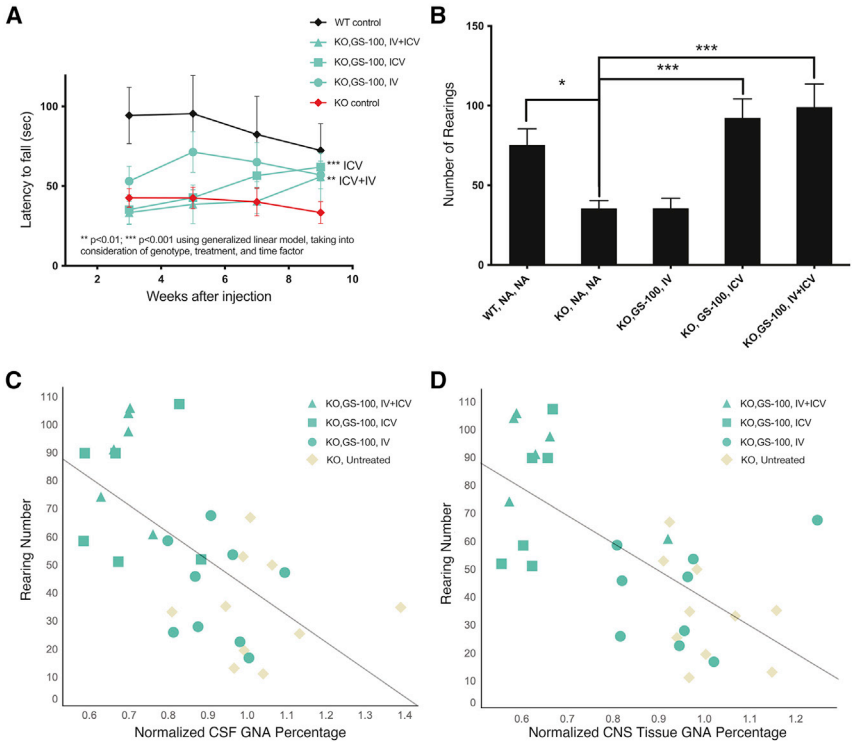

Figure 6. The effect of GS-100 administration via different routes on behavior in *Ngly1*$^{-/-}$ rats and behavioral correlation with GNA levels

(A) GS-100 treatment improved rotarod performance in *Ngl1*$^{-/-}$ rats. The latency on the rotarod was assessed at four time points in WT and *Ngly1*$^{-/-}$ animals treated with GS-100 via IV, ICV, or the dual IV + ICV route. Statistical comparison was performed using the generalized linear model. Each point plotted represents the mean latency per group (minimum N = 4) with error bars representing the SEM. (B) ICV or dual IV + ICV delivery of GS-100 rescued the loss of rearing activity observed in *Ngly1*$^{-/-}$ rats compared with WT rats. Rearing activity was recorded for 15 min at 6 weeks after injection, and the total rearing events were plotted by mean per group with error bars representing the SEM. *p < 0.05, ***p < 0.001. (C and D) Inverse linear correlation between rearing and GNA levels in the CSF (C) or CNS tissues (D) in *Ngly1*$^{-/-}$ animals. Rearing counts were correlated with normalized GNA data taken from CSF after the terminal time point. Left, rearing versus normalized CSF GNA, $R = 0.38$; right, rearing versus tissue GNA, $R = 0.45$. Each data point indicates one rat. GNA, GlcNAc-Asn; KO, knockout; NGLY1, *N*-glycanase 1; WT, wild type.

The results presented here also reinforce that the *Ngly1*$^{-/-}$ rat is a robust animal model for NGLY1 Deficiency. The phenotypes of the *Ngly1*$^{-/-}$ rat model simulate some of the NGLY1 Deficiency patient symptoms, including failure to thrive and a movement disorder that likely stems from CNS issues.[1,4–6] The reversibility of symptoms displayed upon ICV treatment with GS-100 confirms the utility of this model as an *in vivo* platform for evaluating potential therapies.[1,9,12] The phenotypic differences between *Ngly1*$^{-/-}$ and WT rats were consistent, with *Ngly1*$^{-/-}$ rats exhibiting lower body weight and early-onset deficits in coordination and motor function that worsened over time.[18,19] Although NGLY1 protein is ubiquitously expressed across tissue types,[3] many symptoms of NGLY1 Deficiency are related to the CNS and PNS.[3–6] Therefore, the nervous system is believed to have an important role in pathophysiology of NGLY1 Deficiency. This may be related to functional vulnerability of certain CNS cell types to impaired glycoprotein quality control caused by NGLY1 Deficiency, potentially leading to a stress response, motor symptoms, and cognitive impairments.[1,9] The differences between our route of administration study and the study by Asahina et al.[1] include the use of a different AAV9 construct, higher animal number, more routes of administration, and comprehensive correlational analyses between biodistribution, mRNA and protein expression, GNA biomarkers, and behavior. However, the consistency of results between our studies and those of Asahina et al.[1,9] reaffirms that the nervous system is the most relevant primary therapeutic target. Further research is needed to clarify the pathological mechanisms of NGLY1 Deficiency, the role of the CNS and PNS, and the optimal dosing and timing of therapy.[20] No adverse gross or microscopic pathology related to GS-100 were identified in the CNS or periphery and close monitoring of liver function enzymes over time suggests that there is no AAV9-related liver pathology. Together, these findings suggest that GS-100 delivery to the CNS is safe and efficacious in this rat model of NGLY1 Deficiency.

Overall, these results demonstrate that ICV administration of GS-100 was the preferred route of administration, providing widespread delivery and expression of h*NGLY1* DNA, mRNA, and protein in the rat CNS that was associated with GNA biomarker reduction and improved motor function and behavior phenotypes. Based on these results, additional non-clinical studies using ICV administration are being carried out to explore the optimal dose for potential future clinical studies. The correlation between hNGLY1 protein expression and substantial benefit to *Ngly1*$^{-/-}$ rats in the absence of related toxicities supports advancement of GS-100 into the clinic.

MATERIALS AND METHODS

Animals

The Sprague-Dawley *Ngly1*$^{-/-}$ rat was previously generated by deleting approximately 2.6 kb in exon 11 and exon 12 and a 3′ flanking region of the *Ngly1* gene via CRISPR-Cas9 gene editing technology.[9]

Animal care procedures and experiments conformed to the United States Department of Agriculture (USDA) Animal Welfare Act (Code of Federal Regulations, Title 9 [9 CFR], Parts 1, 2, and 3) and are under the strict oversight of the Institutional Animal Care and Use Committee (IACUC), Ethics Committee (EC) and Animal Welfare Body (AWB) at Charles River Labs. Rats were pair-housed where possible. Animals were separated during designated

procedures/activities and as required for monitoring and/or health purposes, as deemed appropriate by the principal investigator and/or clinical veterinarian. Animals were housed in solid-bottom cages with nonaromatic bedding. Fluorescent lighting was provided via an automatic timer for approximately 12 h per day. The basal diet was block Lab Diet Certified Rodent Diet #5002, PMI Nutrition International. Animals were offered HydroGel *ad libitum* during the urinalysis sample collection period. Tap water was offered *ad libitum* to all animals via an automatic water system. Veterinary care was available throughout the course of the study, and animals were examined by the veterinary staff as warranted by clinical signs or other changes. Treatment of the animal(s) for minor injuries or ailments was approved when such treatment did not affect fulfillment of the study objectives.

Animal genotyping

At Charles River Laboratories (CRL), a PCR genotyping assay that targeted the *Ngly1* gene locus was used to differentiate between *Ngly1* WT, *Ngly1*$^{+/-}$, and *Ngly1*$^{-/-}$ rats. All rats were produced as described in Mueller et al.[7]

Generation of *NGLY1*$^{-/-}$ HEK293 cells and ReNcell VM cells

Generation of *NGLY1*$^{-/-}$ HEK293 cells and ReNcell VM cells are described by Mueller et al.[7]

Rat primary neuron culture

To confirm the expression of hNGLY1 protein following GS-100 transduction in neurons, WT primary cortical rat neurons were transduced at varying MOIs and incubated to allow time for cells to express hNGLY1. Fresh E18 rat primary neurons were purchased from Neuromics (PC35102, Edina, MN) and plated following the manufacturer's protocol. Cortical pieces were digested with papain for 30 min at room temperature. Then, the cells were centrifuged at 1,000 rpm for 2 min and resuspended in Neurobasal medium + 10% B27 supplement. Following resuspension, the neurons were plated in 24-well plates at a density of 100,000 cells/well. The neurons were transduced with GS-100 and harvested either at day 10 (MOI 4×10^4 or 8×10^4 vg/cell) or day 15 (MOI 4×10^4 vg/cell). NGLY1 protein detection was performed using western blot with a primary antibody (alpha-hNGLY1) that recognizes the human NGLY1 protein but not the endogenous rat NGLY1 protein.

ReNcell culture

To further confirm the expression of hNGLY1 by GS-100 in human neurons, the human cell line ReNcell VM was transduced with GS-100. ReNcell VM is an immortalized human neural progenitor cell line with the ability to readily differentiate into neurons and glial cells.[21] Undifferentiated ReNcell VM cells were grown on poly-D-lysine and laminin coated T-25 flasks in ReNcell VM NSC Maintenance Medium (SCM005, Millipore) with 20 ng/mL of human recombinant fibroblast growth factor basic protein (bFGF) (GF003, Millipore), human recombinant epidermal growth factor protein (EGF) (GF144, Millipore), and penicillin-streptomycin (15140122, Thermo Fisher). Medium was replaced every other day. ReNcell VM cells were split at >80% confluency. ReNcell VM neuron differentiation is initiated by removing medium with growth factors. GS-100 was added to the medium at 5 days after differentiation at 0, 200,000, and 400,000 MOI.

AAV production

The recombinant AAV9 GS-100 product was produced using the manufacturer's protocol by transient triple transfection of a HEK293 cell line (Vigene Bio, Rockville, MD).

qPCR analysis of biodistribution and mRNA expression

Frozen tissue was dissected into 5- to 25-mg pieces and processed according to manufacturer's protocols using the Qiagen DNeasy or RNeasy Blood and Tissue Kit (69,506 or 74,106). For biodistribution analysis, qPCR was performed on purified DNA using primers targeting the promoter region of the viral genome: forward, 5′- ACGTCA ATGGGTGGAGTATTTACGG;, reverse, 5′-ATGCCAGGCGGGC CATTTAC. Samples were quantified using a NanoDrop One-C (Thermo Scientific) and diluted to 5 ng/μL total DNA in a 50-μL qPCR reaction. A standard curve made from linearized plasmid viral GS-100 vector was run on each plate and viral genomes for each sample were extrapolated. Final calculations were made based on the rat golden path genome size to determine vector copies compared with total diploid genomes. For GS-100 hNGLY1 expression analysis, purified RNA was treated with Qiagen's RNase-Free DNase Set (79254), diluted to 5 ng/μL and reverse transcribed with SuperScript IV VILO (11756050) per manufacturer's protocols. cDNA was amplified using primers targeting the downstream untranslated region of the viral expression cassette forward, 5′-TGGCTGCTCGCCTGTGTTGC; reverse, 5′-CGAAGGCGAAGACGCGGAAGAG, and were normalized to housekeeping gene primers for Hprt1 from IDT DNA (assay number Rn.PT.39a.22214832, RefSeq: NM_012583). All qPCR used Power SYBR Green Master Mix (Thermo 4368706) and were analyzed on an Analytik Jena qTOWER 2.2 Real Time qPCR instrument. After the last cycle, melt temperatures were taken to ensure amplification of a single amplicon.

Quantitative GNA measurements

To prepare samples from cell lines, NGLY1-deficient cells were diluted down to 0.5×10^6 to 2×10^6 cells, pelleted, and analyzed for GNA. The calculated GNA concentration per cell count was averaged across at least two samples and compared between control and NGLY1-deficient cells.

Terminal CSF was collected by ICM puncture, drawn with a syringe, frozen, and later analyzed. Plasma samples were isolated from blood taken via the sublingual vein (in-life collections) or cardiac puncture (terminal collection). Tissue samples were taken upon sacrifice without perfusion. Samples were frozen, dissected to 20- to 50-mg pieces while frozen, homogenized, and analyzed.

Prepared samples were analyzed as described.[7] Briefly, samples were homogenized in PBS, mixed with internal standard and acetonitrile,

and centrifuged. An aliquot of each supernatant was separated via high-pressure liquid chromatography (HPLC) (Shimadzu VP Series 10 System) and analyzed via tandem mass spectrometry (MS/MS) (Applied Biosystems/MDS SciEx API 4000). Detection and accuracy were assessed in surrogate matrices (PBS + BSA, charcoal stripped serum). Each surrogate matrix was spiked with 30 or 300 ng/mL of GNA, processed, and analyzed to determine recovery and accuracy.

GS-100 administration (route of administration study)

GS-100 was administered once on postnatal day 1 (PND ~35–49). Animals treated with both routes of administration were first dosed IV and then ICV on the same day. Animals that received both IV and ICV injection were dosed no more than 4 h apart. Intravenous doses were administered via bolus injection into the tail vein. Respective doses were based on the most recent individual body weights.

GS-100 or vehicle was administered stereotaxically while the animals were under isoflurane (1.5%–2%) anesthesia. GS-100 or vehicle was injected via a Hamilton syringe into lateral cerebral ventricle using the following (or similar) coordinates relative to bregma: Anterior-Posterior (AP), 0.8 mm (caudal); Medial-Lateral (ML), 1.2 mm lateral (right); and Dorsal-Ventral (DV), −4.5 mm from the skull. Then 30 μL of GS-100 or vehicle was injected at a rate of 7 μL per minute. The needle was left in place for at least 2 min and then retracted slowly. The skin incision was closed using standard techniques with any combination of absorbable sutures, staples, wound clips, and/or tissue adhesive. After surgery, the animals were monitored for up to 24 h.

Western blot

To prepare protein samples from cell culture, cells on culture plates were lysed with RIPA buffer (PI89900, Thermo Fisher) containing 1:100 protease/phosphatase inhibitor cocktail (Halt Protease Inhibitor Cocktail, Thermo Fisher) and 5 mM EDTA (03690-100ML, Millipore). The lysate was then vortexed and left on ice for 15 min to digest. To prepare protein samples from tissue, 20–50 mg of tissue was dissected and lysed with RIPA buffer containing 1:50 protease/phosphatase inhibitor cocktail. The lysate was homogenized with a motorized pestle mixer (UX-44468-25, Argos Technologies) for 20 s until no tissue was visible and then left on ice for 15 min to digest. After digestion, the lysate was centrifuged at 10,000 rpm for 10 min and the pellet was discarded. The protein concentration was measured with a BCA assay (PI23227, Thermo Fisher) and run on NuPAGE 4%–12% Bis-Tris Protein Gels (NP0336BOX, Thermo Fisher), before transfer onto a nitrocellulose membrane (LC2001, Thermo Fisher). The membrane was blocked in TBS buffer that contained 5% non-fat milk and 0.5% Tween 20 (97062-332, VWR International) for 1 h. After blocking, the membrane was incubated with rabbit anti-NGLY1 polyclonal antibody (1:1,000, HPA036825, Millipore-Sigma) or mouse anti-GAPDH monoclonal antibody (1:10,000, MAB374, Millipore) overnight at 4°C. Then, the membrane was incubated with Cy5-conjugated goat anti-rabbit secondary antibody (PA45011, GE/Cytiva) or Cy3-conjugated goat anti-mouse secondary antibody (PA43009, GE/Cytiva) for 1 h at room temperature. After 1 h, the protein bands were visualized with an ECL imager (GE/Cytiva). In some experiments, the membrane was incubated with goat horseradish peroxidase (HRP)-conjugated anti-rabbit antibody (AP307P, Millipore) and SuperSignal HRP substrate (PI34577, Thermo Fisher) was used to detect HRP signal. The bands were visualized with an ECL imager (GE/Cytiva). Raw blot data are available upon request.

IHC

Formalin-fixed 5-μm tissue slices from the spinal cord, DRG, and brain tissue of *Ngly1*$^{-/-}$ animals treated with GS-100 (either after ICV or IV, or IV + ICV administration) were incubated with anti-NGLY1 antibody and visualized with 3′3-diaminobenzidine staining (DAB; brown). Hematoxylin nuclear staining (blue) was used as a counterstain. Samples were analyzed for human NGLY1 protein expression using an antibody specific for detecting human NGLY1. IHC optimization was performed on formalin-fixed paraffin-embedded (FFPE) rat tissues using a Leica Bond automated immunostainer and rabbit anti-NGLY1 antibody (HPA036825, Millipore-Sigma). Heat-induced antigen retrieval was performed using Leica Bond Epitope Retrieval Buffer 1 (Citrate solution, pH 6.0) for 20 min. Endogenous peroxidase was blocked using BloxAll (SP-6000, Vector Labs) for 20 min. Non-specific antibody binding was blocked using Novolink Protein Block (RE7280-CE, Leica) for 30 min. Primary antibody was applied for 60 min at room temperature. Anti-rabbit Poly-HRP-IgG secondary antibody (RE7280-CE, lot 6058461, Leica) was applied for 20 min. Anti-NGLY1 antibody was detected using Novocastra Bond Refine Polymer Detection and visualized with DAB (brown). A hematoxylin nuclear counterstain (blue) was applied.

The number of hNGLY1-positive cells and total number of nuclei for each brain region were segmented, annotated, and quantitated using proprietary software (Image DX, Reveal Biosciences, San Diego).

Immunofluorescence in ReNcell VM culture

ReNcells were fixed in warm culture medium containing 4% paraformaldehyde for 15 min. After permeabilization with PBS containing 0.1% Triton X-(100504-970, VWR) for 15 min, the fixed cells were washed and blocked with PBS containing 10% normal goat serum (016201, Fisher Scientific) for 1 h. Afterward, fixed cells were incubated with rabbit anti-NGLY1 antibody (1:100, HPA036825, Millipore-Sigma) and mouse anti-MAP2 antibody (1:100, 13-1500, Thermo Fisher) overnight at 4°C. The cells were then incubated with Alexa goat anti-rabbit 594 fluorescence antibody (1:500, A-11012, Thermo Fisher) and Alexa goat anti-mouse 488 fluorescence antibody (1:500, A28175, Thermo Fisher) for 1 h at room temperature. After, the cells were washed and Hoechst 33342 (1:2,000, H3570, Thermo Fisher) was added to stain the nucleus. The stained cells were imaged on a ZOE Fluorescent Cell Imager (Bio-Rad).

Animal blood, CSF, and tissue collection

In-life blood samples (0.3–0.5 mL) were taken by tail vein. The whole blood was stored on wet ice or ice block until centrifuged. Terminal blood was taken via cardiac puncture.

CSF samples were taken from the cisterna magna under isoflurane sedation and stored on ice block or wet ice following collection until final storage (frozen at −60°C to −90°C).

Tissues were collected at necropsy. Half of tissues were snap frozen in liquid nitrogen and the other half were preserved in 10% neutral buffered formalin. Brains were collected by hemispheres: left hemisphere snap frozen in liquid nitrogen and the right hemisphere was collected for histology. Fixed tissue samples were kept in 10% neutral buffered formalin and transferred to 70% ethanol for up to 72 h prior to processing.

Samples of each tissue were dissected, weighed, and frozen separately −60°C to −90°C until analysis. A 2- to 3-mm tail snip sample was collected from all animals on study and placed into additive-free 1.1-mL Axygen Mini Tubes (MTS-11-8-C) and stored at −10°C to −30°C.

Rotarod and locomotor testing

The accelerating rotarod test is designed to measure balance, coordination, physical condition, and motor learning.[18,22] Rats underwent rotarod testing using the Fusion v6 Rotating Rod System. Conditioning sessions were performed on the morning of or a day prior to the actual testing and involved the animal being placed on the rotarod set to a constant speed of −4 rpm (the minus sign indicates that the rod is moving in a direction that causes the rat to ambulate away from the observer) for 4 min. During the actual test, animals were placed on a rotating rod programmed to accelerate from 4 to 40 rpm at a rate of 0.15 revolutions per second over the course of 4 min. For animals staying on the rotarod for the entire 4-min period, a time of 240 s was recorded as the fall time. The elapsed time from the start of the trial to the animal's fall was recorded digitally by the instrument. Each animal was evaluated in three trials with at least 15 min between trials. The average of all three trials is reported for each animal.

Locomotor testing was performed by placing the animals into a Hamilton-Kinder enclosure. The duration of monitoring of rearing activity was 15 min. General linear model (JMP software) with genotypes, time point, and route of administration as effects was used for statistical analysis comparing the averaged fall time (rotarod) and rearing activity for rotarod and locomotor, respectively.

In the characterization study, FOB testing was conducted on all animals without knowledge on the part of the testers of the treatment status of each animal. Each animal was observed for a minimum of 3 min in a black Plexiglas open-field observation box. Parameters evaluated were based on those outlined by Moser and coworkers.[13,14]

Overview of the characterization study and the route of administration study

The characterization study of a KO rat model of NGLY1 Deficiency included evaluation of autonomous functions, motor function, and locomotor activity conducted over 22 weeks. Functional assessments, rotarod, and FOB were conducted every 2 weeks throughout the study.

To determine the optimal route of administration of GS-100 in *Ngly1*$^{-/-}$ rats, the route of administration study evaluated the *in vivo* biodistribution and expression of human NGLY1 by GS-100 in rat primary neurons; the reduction of GNA in blood, urine, and CSF after GS-100 treatment; and the effects of GS-100 on behavior in *Ngly1*$^{-/-}$ rats. The dose (6×10^{12} vg total or 4×10^{10} vg/μL CSF) was chosen to conform to previous AAV9 ICV administration.[2,10] Blood and CSF samples were collected at baseline; weeks 2, 4, and 6 post injection; and at termination for clinical chemistry and biomarkers. Rotarod assessment were conducted at weeks 3, 5, 7, and 9, and open-field rearing activity was assessed at week 6, 7, and 9. After necropsy, fixed CNS and selected peripheral tissues were FFPE embedded, sliced, stained with hematoxylin and eosin, and evaluated by a certified pathologist. Tissue samples were collected and one hemibrain was frozen and later dissected for biodistribution, mRNA expression, and western blot analysis.

In vitro validation of the NGLY1 gene therapy candidate, GS-100

We developed GS-100, a recombinant single-stranded AAV9 vector encoding a codon-optimized full-length version of the human *NGLY1* gene for the treatment of NGLY1 Deficiency.

To confirm the expression of hNGLY1 by GS-100 in human neurons, the human cell line ReNcell VM (Ventral Mesencephalon) was transduced with GS-100. ReNcell VM is an immortalized human neural progenitor cell line with the ability to readily differentiate into neurons and glial cells.

NGLY1$^{-/-}$ cells were previously shown to have higher levels of the NGLY1 substrate (GNA) compared with WT controls.[7,8,23] To determine whether GS-100 can restore functional NGLY1 protein in *NGLY1*$^{-/-}$ cells and reduce their abnormally high GNA levels, we transduced *NGLY1*$^{-/-}$ HEK293 cells with GS-100 and analyzed the level of GNA in the cell lysate using mass spectrometry.

In vivo validation of NGLY1 gene therapy in *Ngly1*$^{-/-}$ rats and optimal route of administration

The rats were assessed for physiological and behavioral impacts of GS-100 longitudinally before being taken down for analysis of biodistribution, gene expression, and GNA analysis 9 weeks after dosing.

The highest ICV dose of AAV9 reported in mice to our knowledge is described by Hocquemiller et. al..[10] Hirai et al. used 2.4×10^{14} vg total in their intrathecal injection which is equivalent to a dose of 6.9×10^{10} VG/μL CSF[17] (assuming CSF volume of 35 μL for mice). Based on CSF volume (assuming rat CSF volume of 150 μL), this corresponds to a maximum dose of 1.0×10^{13} vg total in rats. A slightly lower dose of 6×10^{12} VG (or 4×10^{10} VG/μL of CSF) was used in our study due to volume dosing safety limitations (up to 30 μL per rat) and AAV9 concentration constraints (at least 2×10^{14} VG/mL).

WT and KO rats were divided into seven groups with either n = 4 or n = 8 (sex balanced in either case). Group 1 (*Ngly1*$^{-/-}$; n = 8) and group

7 (WT; n = 8) were untreated animals; groups 4–6 (n = 8 in each group) were *Ngly1*$^{-/-}$ rats dosed with 1×10^{14} vg/kg of GS-100 via IV, 6×10^{12} vg/animal via ICV, and 6×10^{12} vg/animal (ICV) plus 1×10^{14} vg/kg GS-100 via the IV + ICV route respectively; group 2 (n = 4) were *Ngly1*$^{-/-}$ rats dosed with vehicle via the IV + ICV route; group 3 (n = 4) were WT rats dosed with GS-100 via the IV + ICV route. The volume for all ICV dosing is 30 μL. At the end of the study, CNS and peripheral tissues were collected and assessed for *hNGLY1* DNA biodistribution via qPCR.

To determine whether transduction of GS-100 resulted in hNGLY1 expression, we analyzed hNGLY1 mRNA in the CNS of the different treatment groups.

Human NGLY1 protein expression in brain detected by IHC

To determine the protein expression pattern of the hNGLY1 transgene in the CNS and peripheral tissues, paraffin-embedded brain slices were stained for hNGLY1 protein by IHC.

To further understand GS-100-dependent hNGLY1 protein expression in different brain regions, the hNGLY1-positive cells in each brain region were segmented, annotated, quantitated, and normalized to the total number of nuclei. The hNGLY1-positive cell ratio was calculated by normalizing the number of hNGLY1-positive cells to the total number of nuclei for each brain region.

GNA biomarker levels decrease in CSF, blood, and tissues following GS-100 dosing

To determine whether GNA accumulation could be reduced by GS-100 treatment, we compared GNA levels in treated versus untreated *Ngly1*$^{-/-}$ rats. In addition to plasma and CSF samples, tissue samples were analyzed for GNA biomarker content. To further investigate the relationship between GS-100 transduction, hNGLY1 expression, and GNA reduction, we plotted the data from the thalamus and hippocampus for correlation (Figures 5A–5F).

Amelioration of motor and neurobehavioral deficits after GS-100 ICV administration

Motor and neurobehavioral responses to GS-100 administration were measured in the rotarod and open-field tests. Spontaneous rearing behavior in an open-field environment is a measurement of exploratory behavior and general motor function in rodents.[24]

Data availability statement

Data available upon request for non-commercial purposes, without breaching participant confidentiality.

SUPPLEMENTAL INFORMATION

Supplemental information can be found online at https://doi.org/10.1016/j.omtm.2022.09.015.

ACKNOWLEDGMENTS

Medical writing support was provided by Patricia Rawn and Judy Wiles of Facet Communications and funded by Grace Science, LLC. The characterization study was funded by the Grace Science Foundation and the route of administration study was funded by Grace Science, LLC.

AUTHOR CONTRIBUTIONS

L.Z., W.M., T.W., S.D., B.B., and B.C. designed experiments. B.C. designed GNA experiments. L.Z., W.M., T.W., S.D., and B.B. designed the animal studies. L.Z., W.M., T.W., S.D., B.B., and M.F.W. managed the animal studies. L.Z. and W.F.M. analyzed the animal studies. W.F.M. managed and analyzed biomarker studies. L.Z., W.F.M., B.T., and J.W.C. performed the *in vitro* studies and analysis. L.Z., W.F.M., S.D., M.W., B.E.C., J.W.C., and B.S. wrote the paper.

DECLARATION OF INTERESTS

L.Z., B.T., S.D., B.B., M.F.W., T.W., B.S., J.W.C., and W.F.M. are or were employees of Grace Science, LLC. B.E.C. is a consultant for Grace Science, LLC.

REFERENCES

1. Asahina, M., Fujinawa, R., Hirayama, H., Tozawa, R., Kajii, Y., and Suzuki, T. (2021). Reversibility of motor dysfunction in the rat model of NGLY1 deficiency. Mol. Brain *14*, 91. https://doi.org/10.1186/s13041-021-00806-6.

2. NORD (2021). NGLY1 deficiency. https://rarediseases.org/rare-diseases/ngly1-deficiency/#:~:text=NGLY1%20deficiency%20is%20caused%20by,NGLY1%20deficiency%20have%20been%20identified.

3. Suzuki, T., Huang, C., and Fujihira, H. (2016). The cytoplasmic peptide:N-glycanase (NGLY1) - structure, expression and cellular functions. Gene *577*, 1–7. https://doi.org/10.1016/j.gene.2015.11.021.

4. Lam, C., Ferreira, C., Krasnewich, D., Toro, C., Latham, L., Zein, W.M., Lehky, T., Brewer, C., Baker, E.H., Thurm, A., et al. (2017). Prospective phenotyping of NGLY1-CDDG, the first congenital disorder of deglycosylation. Genet. Med. *19*, 160–168. https://doi.org/10.1038/gim.2016.75.

5. Abuduxikuer, K., Zou, L., Wang, L., Chen, L., and Wang, J.S. (2020). Novel NGLY1 gene variants in Chinese children with global developmental delay, microcephaly, hypotonia, hypertransaminasemia, alacrimia, and feeding difficulty. J. Hum. Genet. *65*, 387–396.

6. Caglayan, A.O., Comu, S., Baranoski, J.F., Parman, Y., Kaymakçalan, H., Akgumus, G.T., Caglar, C., Dolen, D., Erson-Omay, E.Z., Harmanci, A.S., et al. (2015). NGLY1 mutation causes neuromotor impairment, intellectual disability, and neuropathy. Eur. J. Med. Genet. *58*, 39–43. https://doi.org/10.1016/j.ejmg.2014.08.008.

7. Mueller, W.F., Zhu, L., Tan, B., Dwight, S., Beahm, B., Wilsey, M., Wechsler, T., Mak, J., Cowan, T., Pritchett, J., et al. (2022). GlcNAc-Asn (GNA) is a biomarker for NGLY1 deficiency. J. Biochem. *171*, 177–186. https://doi.org/10.1093/jb/mvab111.

8. Haijes, H.A., de Sain-van der Velden, M.G.M., Prinsen, H.C.M.T., Willems, A.P., van der Ham, M., Gerrits, J., Couse, M.H., Friedman, J.M., van Karnebeek, C.D.M., Selby, K.A., et al. (2019). Aspartylglycosamine is a biomarker for NGLY1-CDDG, a congenital disorder of deglycosylation. Mol. Genet. Metabol. *127*, 368–372. https://doi.org/10.1016/j.ymgme.2019.07.001.

9. Asahina, M., Fujinawa, R., Nakamura, S., Yokoyama, K., Tozawa, R., and Suzuki, T. (2020). Ngly1 -/- rats develop neurodegenerative phenotypes and pathological abnormalities in their peripheral and central nervous systems. Hum. Mol. Genet. *29*, 1635–1647. https://doi.org/10.1093/hmg/ddaa059.

10. Hocquemiller, M., Giersch, L., Audrain, M., Parker, S., and Cartier, N. (2016). Adeno-associated virus-based gene therapy for CNS diseases. Hum. Gene Ther. *27*, 478–496. https://doi.org/10.1089/hum.2016.087.

11. Hudry, E., and Vandenberghe, L.H. (2019). Therapeutic AAV gene transfer to the nervous system: a clinical reality. Neuron *101*, 839–862. https://doi.org/10.1016/j.neuron.2019.02.017.

12. Fujihira, H., Masahara-Negishi, Y., Tamura, M., Huang, C., Harada, Y., Wakana, S., Takakura, D., Kawasaki, N., Taniguchi, N., Kondoh, G., et al. (2017). Lethality of mice bearing a knockout of the Ngly1-gene is partially rescued by the additional deletion of the Engase gene. PLoS Genet. *13*, e1006696. https://doi.org/10.1371/journal.pgen.1006696.

13. Moser, V.C., McCormick, J.P., Creason, J.P., and MacPhail, R.C. (1988). Comparison of chlordimeform and carbaryl using a functional observational battery*1. Fund. Appl. Toxicol. *11*, 189–206. https://doi.org/10.1016/0272-0590(88)90144-3.

14. Moser, V.C. (1996). Rat strain- and gender-related differences in neurobehavioral screening: acute trimethyltin neurotoxicity. J. Toxicol. Environ. Health *47*, 567–586. https://doi.org/10.1080/009841096161546.

15. Armbruster, N., Lattanzi, A., Jeavons, M., Van Wittenberghe, L., Gjata, B., Marais, T., Martin, S., Vignaud, A., Voit, T., Mavilio, F., et al. (2016). Efficacy and biodistribution analysis of intracerebroventricular administration of an optimized scAAV9-SMN1 vector in a mouse model of spinal muscular atrophy. Mol. Ther. Methods Clin. Dev. *3*, 16060. https://doi.org/10.1038/mtm.2016.60.

16. Perez, B.A., Shutterly, A., Chan, Y.K., Byrne, B.J., and Corti, M. (2020). Management of neuroinflammatory responses to AAV-mediated gene therapies for neurodegenerative diseases. Brain Sci. *10*, E119. https://doi.org/10.3390/brainsci10020119.

17. Hirai, T., Enomoto, M., Kaburagi, H., Sotome, S., Yoshida-Tanaka, K., Ukegawa, M., Kuwahara, H., Yamamoto, M., Tajiri, M., Miyata, H., et al. (2014). Intrathecal AAV serotype 9-mediated delivery of shRNA against TRPV1 attenuates thermal hyperalgesia in a mouse model of peripheral nerve injury. Mol. Ther. *22*, 409–419. https://doi.org/10.1038/mt.2013.247. Epub 2013 Oct 28.

18. Crawley, J.N. (2003). Behavioral phenotyping of rodents. Comp. Med. *53*, 140–146.

19. Buccafusco, J. (2009). Methods of Behavior Analysis in Neuroscience, 2nd Edition (Taylor & Francis Group).

20. Bevan, A.K., Duque, S., Foust, K.D., Morales, P.R., Braun, L., Schmelzer, L., Chan, C.M., McCrate, M., Chicoine, L.G., Coley, B.D., et al. (2011). Systemic gene delivery in large species for targeting spinal cord, brain, and peripheral tissues for pediatric disorders. Mol. Ther. *19*, 1971–1980. https://doi.org/10.1038/mt.2011.157.

21. Donato, R., Miljan, E.A., Hines, S.J., Aouabdi, S., Pollock, K., Patel, S., Edwards, F.A., and Sinden, J.D. (2007). Differential development of neuronal physiological responsiveness in two human neural stem cell lines. BMC Neurosci. *8*, 36. https://doi.org/10.1186/1471-2202-8-36.

22. Curzon, P. (2009). The Behavioral Assessment of Sensorimotor.

23. Mueller, W. (2020). AAV9-Mediated gene therapy for NGLY1 deficiency and assessment of GNA biomarker changes in a rat disease model. Mol. Ther. *28*, 124–125.

24. Sturman, O., Germain, P.L., and Bohacek, J. (2018). Exploratory rearing: a context- and stress-sensitive behavior recorded in the open-field test. Stress *21*, 443–452. https://doi.org/10.1080/10253890.2018.1438405.